Development of a 200 MHz 30 MW Multiple Beam Inductive Output Tube

Final Report

DE-FG02-07ER84912

Calabazas Creek Research, Inc.
690 Port Drive
San Mateo, CA 94404
(650) 312-9575
RLI@CalCreek.com

June 19, 2008

1. Introduction

1.1. Identification and Significance of the Problem or Opportunity, and Technical Approach

RF sources are required for powering accelerators operating at approximately 200 MHz and providing 30 MW for each accelerator cavity. A number of sources can provide this power, including single beam and multiple beam klystrons. Klystrons operate by bunching an electron beam using a series of RF cavities with power extracted from the beam in the final output cavity. Typically, 5-6 cavities are required to provide sufficient bunching for high efficiency and gain, resulting in a large device at MHz frequencies. Efficiencies are typically limited to less than 60%.

A fundamental mode (FM) multiple beam (MB) inductive output tube (IOT) is also a candidate RF source to provide this power. The FM MBIOT offers compactness and improved efficiency. A klystron at this frequency would be extremely large, both in length and diameter; conservatively six meters in length and two meters in diameter, including the focusing magnet. Weight would be measured in tons. A multiple beam klystron (MBK) is also a strong candidate. An MBK could reduce the overall length of the tube by perhaps 50%, and the operating voltage could be reduced by more that a factor of two. The FM MBIOT would be half again smaller; the length of the tube would be less than 25% of the conventional klystron and operate at half the voltage. The weight of the FM MBIOT would drop to 20% of the klystron. The size and weight estimates are based on a comparison of the CPI VKP-7952A klystron and the CPI VHP-8330A higher order mode (HOM) IOT, both of which were designed to operate at 700 MHz center frequency and 1 MW CW. Layout drawings comparing these two sources are presented in Figure 1.

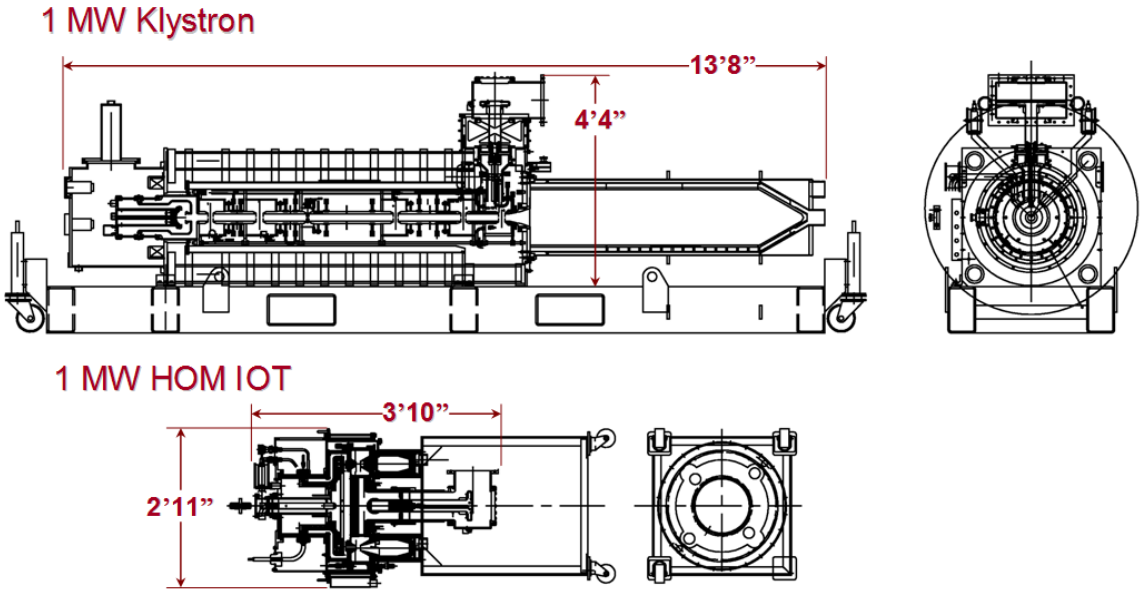

Figure 1. Comparison of a 700 MHz 1 MW klystron and a higher order mode inductive output tube with the same RF power and frequency

The Phase I program determined that a MBIOT could achieve the 30 MW of RF output power with an operating voltage of 100 kV. Table 1 presents the operating parameters as

function of the number of electron beams. The program also explored driver tube technology for the MBIOT. IOTs are relatively low gain devices, and the proposed device will require approximately 200 kW of RF drive power. One option is to design a single beam IOT that operates at the same voltage as the MBIOT on a common power supply. This is common practice for high-power radar transmitters using cross-field amplifier chains.

Table 1. Preliminary parameters for a 30 MW 200 MHZ IOT

Number of Beams	**17**	**17**	**23**	**23**
Beam Voltage (Kv)	110	115	110	115
Total Beam Current (A)	425	408	426	405
Current per Cathode (A)	25	24	18.5	17.6
Available Beam Power (MW)	47	47	47	47
RF Output Power (MW)	30.4	30.5	30.4	30.2

The program built on the experience gained a previous 700 MHz program [1]. The program considered the cost and complexity of the RF source, power supply, driver, and transmission line system.

While the design of the 30 MW MBIOT was successful, analysis of the cost indicated that a device could not be built and tested within the resources of a Phase II SBIR program. Details of the design and cost analysis are presented in this report. Section 2 will describe the Phase I results in detail.

1.2. Anticipated Benefits

Because the IOT achieves beam bunching at the cathode, there are no additional cavities required other than the output cavity. Beam bunching at the cathode is also more efficient, so the performance in enhanced. Consequently, the IOT provides an RF source that is dramatically more compact and efficient than a klystron. In addition, the magnetic circuit can be quite simple and compact, further reducing the cost and complexity. A disadvantage is that the gain is significantly less than can be achieved in a klystron. Where klystron gains can exceed 45 dB, IOT gains are typically limited to 24 dB. This requires additional power from the RF driver of the amplifier.

The increased efficiency and reduced beam voltage offered by the multiple beam IOT makes these sources significantly more compact and less expensive to build and operate than comparable klystrons. This also reduces power supply costs and facilities costs. This cost reduction also extends to the procurement and operating expense of the magnet. Successful development of a multiple beam IOT would provide a new, high performance, RF source for many pulsed power applications.

2. Degree to Which Phase I Demonstrated Technical Feasibility

The technical tasks proposed for the Phase I program were as follows:

- Investigate circuit alternatives, including fundamental mode and higher order mode circuits,

- Design a distributed electron beam to achieve voltage reduction compatible with the optimum circuit design,
- Design the RF windows, input and output couplers, spent beam collector, and magnet,
- Generate a mechanical model of the complete RF source,
- Determine anticipated operating parameters, including power supply and RF driver specifications.

All tasks were successfully completed. A fundamental mode input circuit was designed to drive twenty four electron guns. Analysis of the output cavity indicated that an efficiency of 70% could be achieved producing the required output power of 30 MW pulsed with 23 dB gain. The RF windows, input and output couplers, collector, and magnet were designed and were within design limitations. A mechanical model was generated that demonstrates the compactness of the device. These results indicate that development of a 30 MW multiple beam inductive output tube is clearly feasible.

One issue, however, is the availability of a driver. Since the MBIOT gain is approximately 24 dB, the driver will be required to provide approximately 200 kW. Clearly, there are no solid state drivers available at this power level and frequency. Communications & Power Industries, Inc., the industrial partner on this program, designed an IOT amplifier at the required frequency and power level. A development effort would be required, however, to fully develop this device. Additional information is provided in Section 4.5.

Results of the Phase I program are described below.

2.1. Investigation of Circuit Alternatives

2.1.1. Input Cavity

The initial task was to determine the impact of various numbers of electron guns on the operating parameters. These results were shown in Table 2. Based on this analysis, it was decided to investigate a design incorporating approximately 23 guns and operating at approximately 100 kV. After considering several potential gun arrangements, it was decided to use 24 guns in a double ring arrangement, shown in Figure 2.

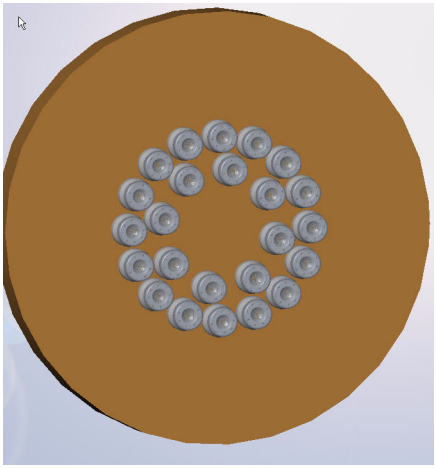

Figure 2. Arrangement of electron guns in input cavity

Design of the input cavity used Ansoft's High Frequency Structure Simulator (HFSS). Many geometries were analyzed before achieving the desired performance. Figure 3 shows a solid

model of the final configuration. The copper colored lines provide current and cooling to

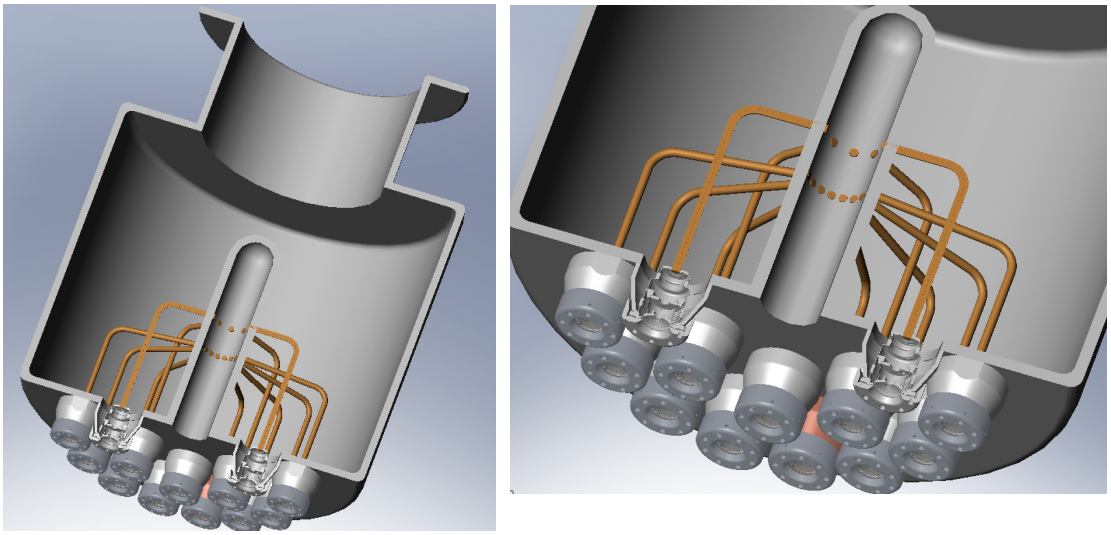

Figure 3. Solid model of the 200 MHz input cavity. The connectors between the electron guns and the center coax provide current to and cooling to the guns.

the individual guns. The unique coaxial configuration allows these connections without disturbance of the input cavity mode.

The proposed IOT would use existing electron guns currently in production. This dramatically reduces the cost, since these guns are produced in fairly large quantities.The design and performance are well documented following years of operation in existing IOTs and klystrodes.

Figure 4 shows a photo of the K2 electron gun stem and the associated HFSS model. In the IOT, the input cavity generates an electric field between the cathode and the grid at the frequency of the input signal. During the positive half cycle of the electric field, the value reaches sufficient magnitude to extract electrons from the cathode. These are then

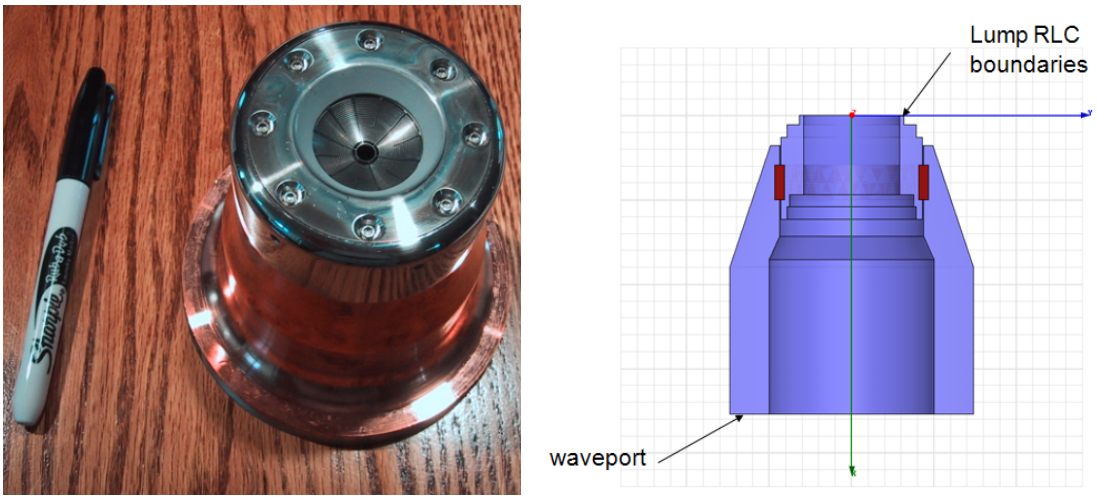

Figure 4. Photograph of a K2 IOT electron gun and the associated HFSS model

accelerated by the anode voltage toward the output cavity. The lumped RLC boundaries on the HFSS model account for the impact of the grid on the field calculations.

Figure 5 shows the input cavity model for HFSS. The eight-fold symmetry reduced the computation time during the initial design. The input power is fed into the cavity through

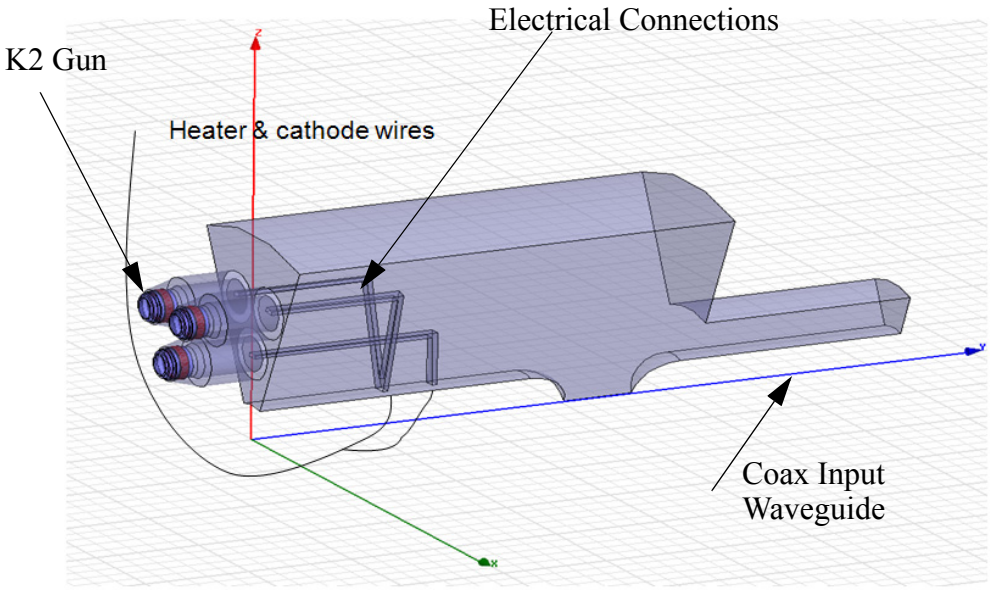

Figure 5. 1/8 Model of MBIOT Input Cavity

a coaxial waveguide on the device axis. This excites a coaxial mode in the cavity. The axial electric field of the mode appears at an accelerating voltage between the grid and cathode.

Figure 6 shows the electric fields in the cavity. Note that the peak electric field appears on the center conductor of the input waveguide. The level is within acceptable limits.

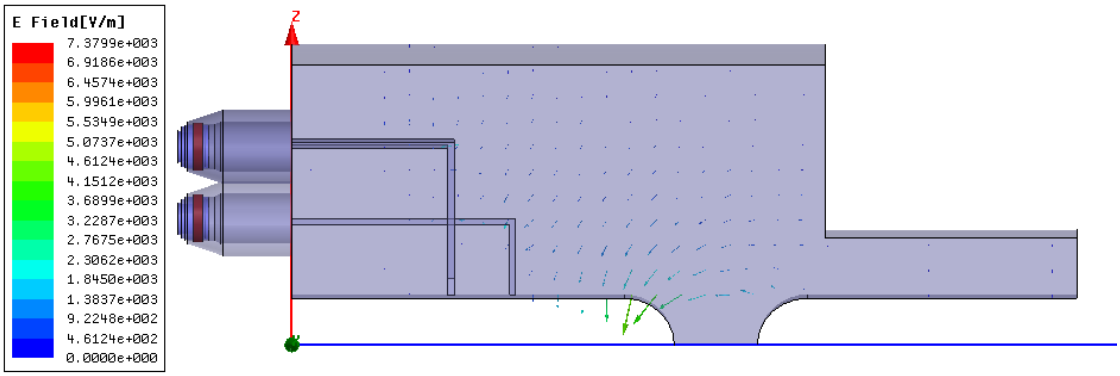

Figure 6. Input cavity electric fields

Figure 7 shows the VSWR of the input cavity as seen by the input drive signal. This indicates the cavity can be well matched to the input driver, though the cavity is slightly

off frequency. Further research would optimize the cavity frequency. If necessary, a tuner could be added to adjust the frequency.

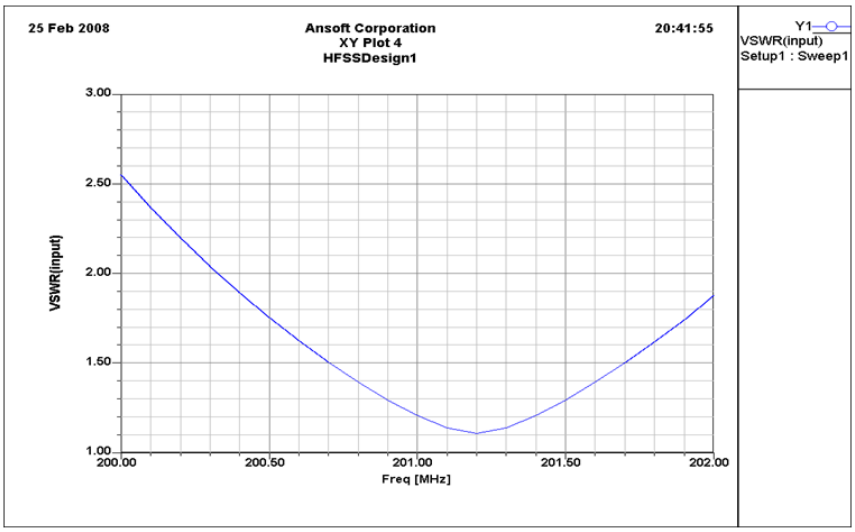

Figure 7. Input cavity VSWR

Figure 8 shows a plot of the electric fields across the cathode-grid gaps of the inner and outer rings of cathodes. Note that they are close to the same values. This plot indicates there will be slightly more current in the outer beams than the inner beams. This should have negligible effect on the IOT performance.

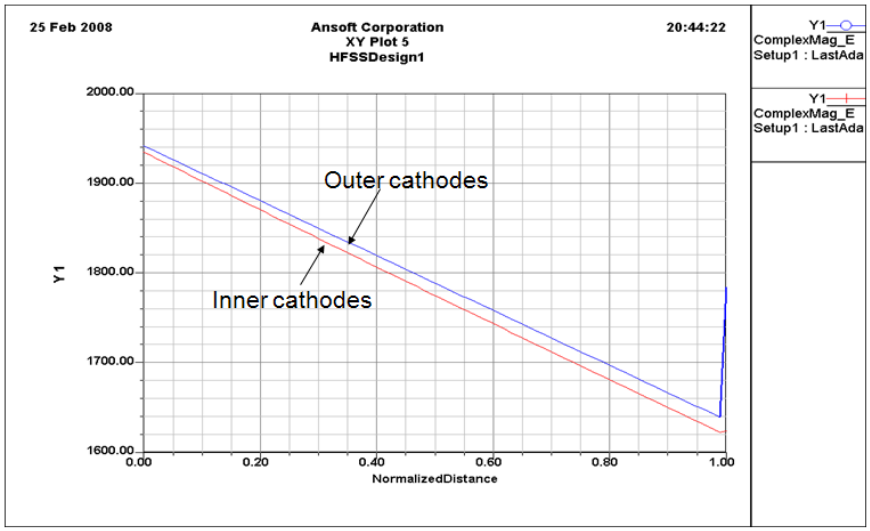

Figure 8. Electric fields at the cathodes

The input cavity geometry represents an innovative design where there is capacitive coupling of the input signal to the cavity and inductive coupling of the fields to the K2 guns. The design shown is matched at 201.5 MHz with a 3 dB bandwidth of 4 MHz. No effort was made in the Phase I program to maximize the bandwidth. The power appears to be equally divided among the 24 cathodes. An RF choke will be required to maintain the

input coax waveguide at ground potential while the cavity is energized to the operating voltage of 100 kV.

2.1.2. Output Cavity

The geometry of the output cavity is shown in Figure 9. The HFSS model shows the vacuum regions in the simulation, and the solid model shows the actual mechanical design. One of the seven beam lines is shown sliced. The output power is extracted from a single coaxial output coupler on the axis. HFSS modeled the electric fields and determined the resonant frequency, R/Q, and the output coupling.

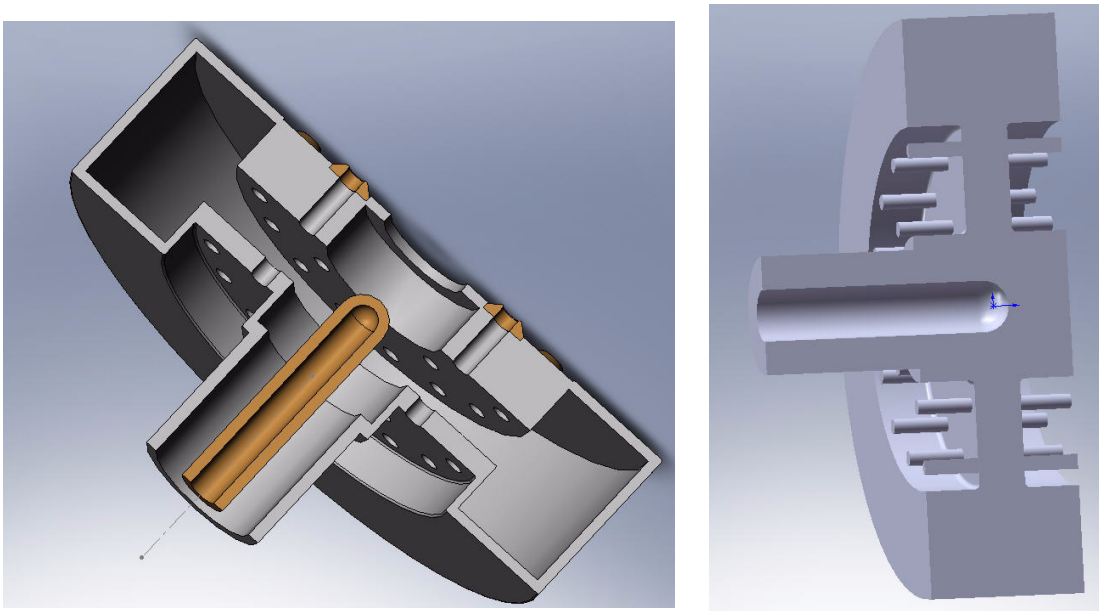

Figure 9. Output cavity geometry. The left view is a solid model. The right view is the HFSS model showing vacuum regions used in the simulation.

Figure 10 shows the simulation of the electric fields in the output cavity at one phase of the RF cycle. Peak electric field occurs at the location of the electron beams, as desired.

The final simulated results for the output cavity performance are presented in the table below. The MBIOT is predicted to achieve all required performance parameters.

The Phase I program did not attempt to maximize the MBIOT bandwidth.

Table 2: Predicted MBIOT Performance

Parameter	Value		Parameter	Value
R/Q (Ohms)	30		Number of beams	24
Gap Length (in.)	1.57		Unloaded Output Cavity Q	11000
Beam Diameter (in.)	0.33		Unloaded Input Cavity Q	5000
Tunnel Diameter (in.)	1.0		Tunnel Length anode to gap (in.)	2.75
Frequency (MHz)	200		Beam Voltage (kV)	99

Table 2: Predicted MBIOT Performance

Parameter	Value		Parameter	Value
Grid bias voltage (V)	210		Drive Power (kW)	123
Total Beam Current (A)	425		Peak Emission density (W/cm^2)	7.6
Output Power (MW)	31.0		Efficiency (%)	73.7
Gain (dB)	23.9		Output cavity loss (W)	283
Loaded output Q	114		-3 dB Bandwidth (MHz)	1.8

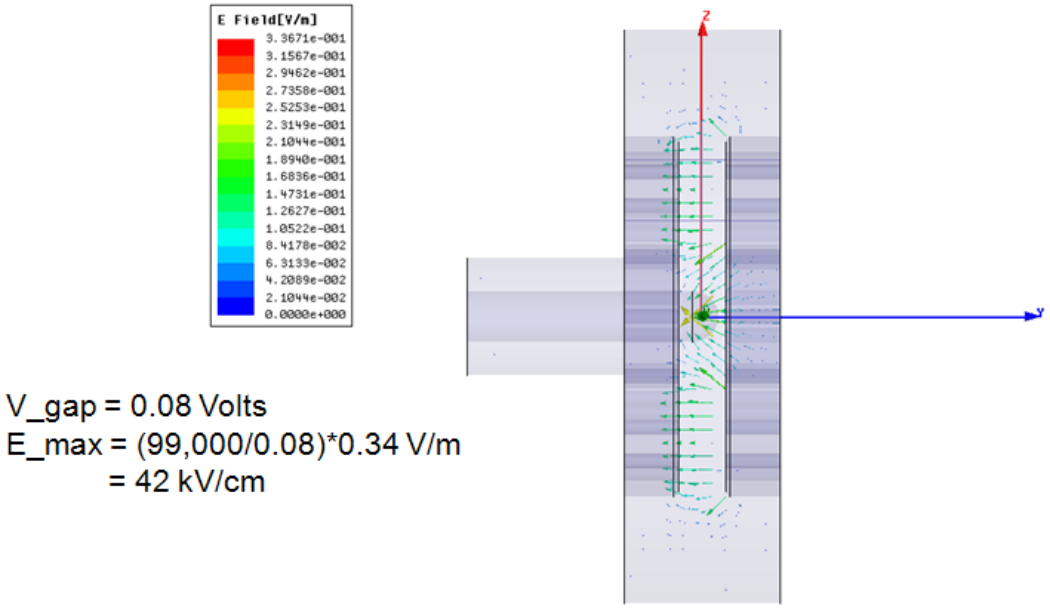

Figure 10. HFSS simulation of output cavity

2.2. Design a distributed electron beam to achieve voltage reduction compatible with the optimum circuit design

Twenty four electron guns provide the beam power for the output cavity. Figure 11 shows a slice through the gun geometry showing details of one gun. As previously mentioned, the input cavity imposes a sinusoidal voltage between the grid and cathode at the RF drive frequency. The guns are radially spaced from the center of the device and the axis of the magnetic field, so 3D simulations are required. Also, since the grid-cathode voltage is varying with the RF frequency, the extracted current from the cathode is also varying. Consequently, the beam optics can only be ideally designed for a single grid voltage and beam current. Other values of these parameters result in non-ideal beams; however, this does not have an appreciable impact on the performance as long as beam transmission is achieved for all values of the current.

Figure 12 shows beam trajectories for one of the electron guns in the outer row. Since the beam current is dependent on the phase of the input RF signal, plots of different current

values are shown. Note that full beam transmission is easily achieved for all current

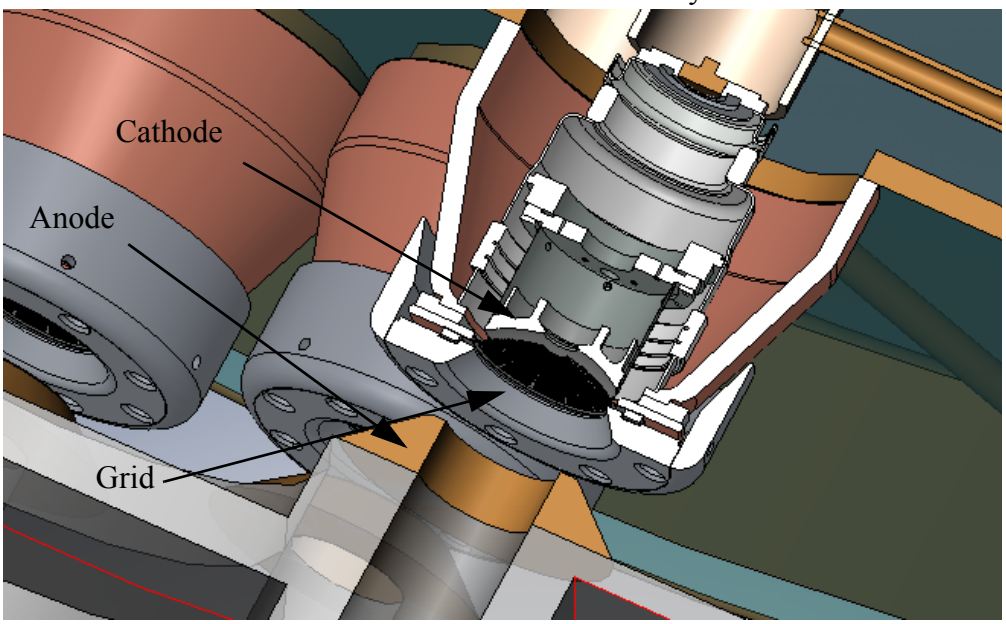

Figure 11. Sliced view of one of twenty four electron guns

values. A similar result is shown for simulation of one of the inner beams in Figure 13

.

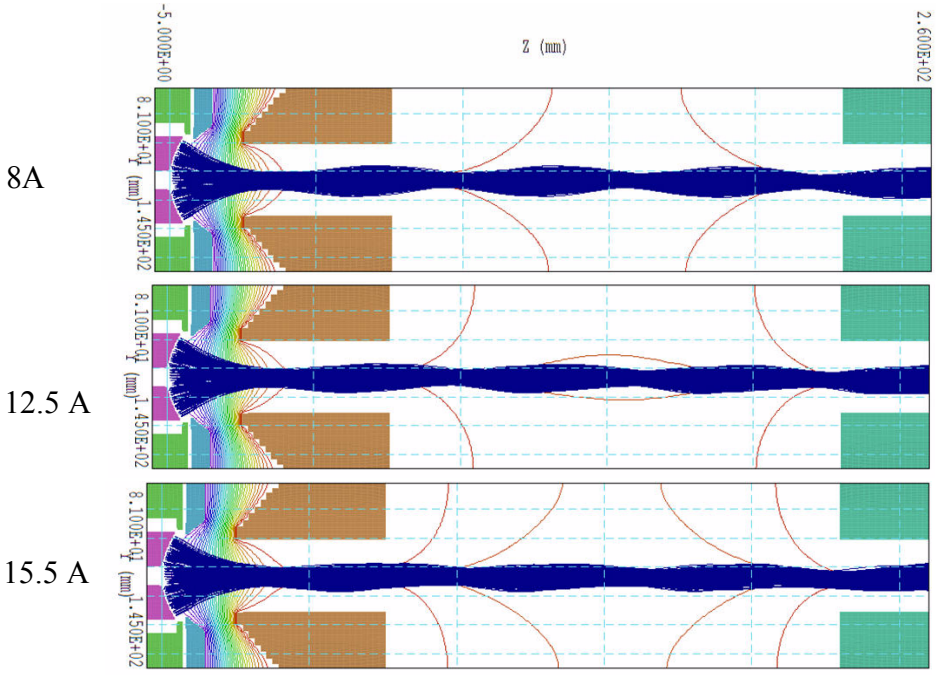

Figure 12. Outer beam trajectories at various currents

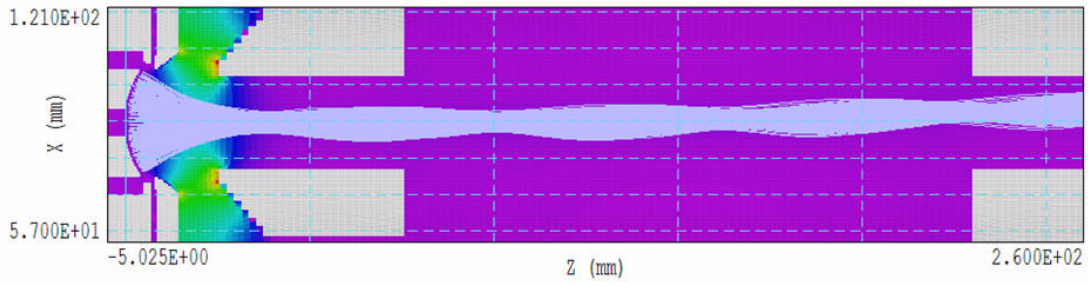

Figure 13. Simulation of inner electron beam at 12 A

Magnetic focusing for IOTs consists primarily of a flat magnetic field between the polepieces of a single coil magnet (described later). These guns essentially are Brillouin focused, since confined flow focusing would be extremely complex for off-axis guns.

Electric field gradients in the gun were analyzed to insure acceptable limits were not exceeded for pulsed operation. Figure 14 shows a simulation in Beam Optics Analysis showing electric field contours for 150 kV operation, well above the expected requirement. These results were also confirmed with OnmiTrak.

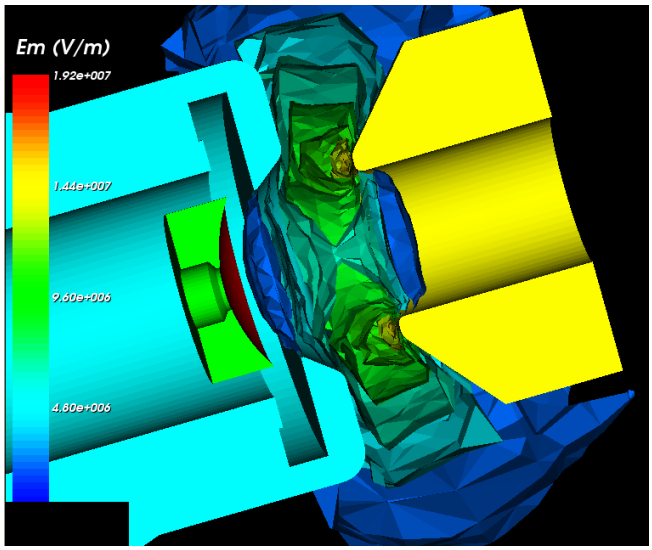

Figure 14. Field gradient analysis plot from Beam Optics Analysis at 150 kV

Because the electron guns are spaced much further apart then the cathode to anode distance, there is no interaction between beams in this region. The only potential interaction occurs in the output cavity, where the magnetic field confines each beam.

This analysis indicates that design of the electron gun for the multiple beam IOT should be relatively simple and robust. Each beam line is essentially that of a single beam IOT using a well establish, production electron gun.

2.3. Design the RF windows, input and output couplers, spent beam collector, and magnet

2.3.1. Input Window

The RF input power is fed into the input cavity through a single, coaxial waveguide on the axis of the MBIOT. A solid model of the geometry is shown in Figure 15. The center conductor is stepped before and after the window ceramic to provide the required match at the operating frequency. The ceramic is 99.5% pure alumina approximately 1.4 inches thick. This represents a very robust mechanical design. If necessary, water cooling channels will be incorporated into the center conductor.

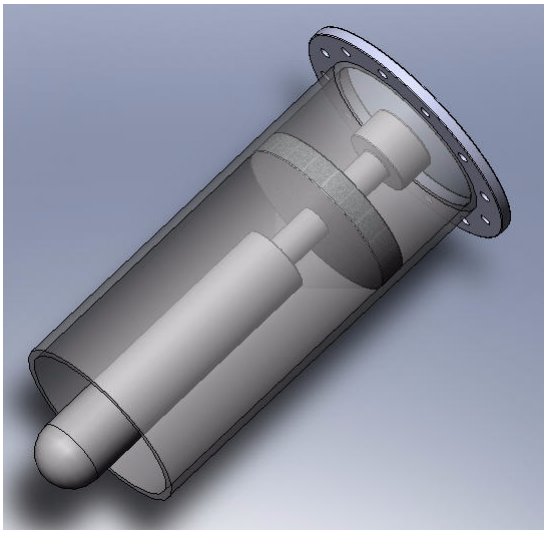

Figure 15. Solid model of input window

The window design was designed using CCR's CASCADE program, which includes on optimizer for achieving an optimal configuration. Results were also confirmed using HFSS. CASCADE is a mode matching code used throughout the microwave tube industry and is well validated. The VSWR is predicted to be less than 1.005 at the operating frequency of 200 MHz. Also note the extremely large bandwidth of the window.

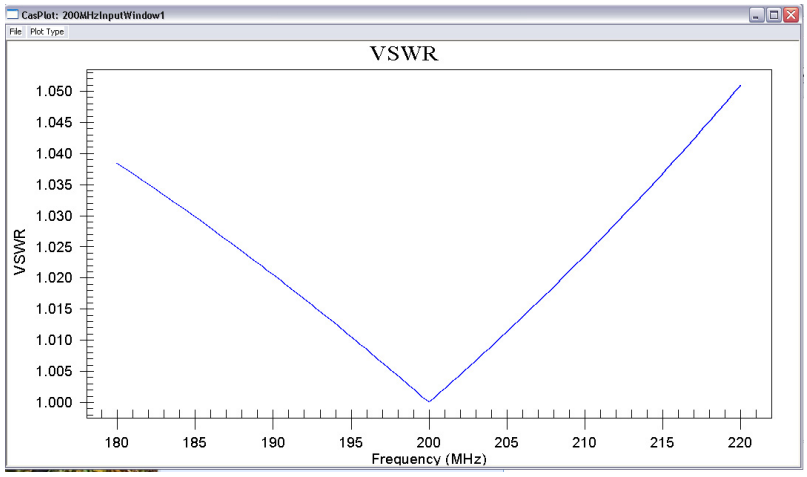

Figure 16. Input window VSWR from CASCADE (left) and HFSS (right)

CASCADE can also search for ghost or trapped modes in the geometry. None were found near the operating frequency of the MBIOT.

2.3.2. Output Window

The geometry of the output window is similar to that of the input window and is shown in Figure 17. This window also uses high purity alumina ceramic that is approximately 01.5 inches thick. This represents a very robust design at this frequency and power level.

As before, the performance was modeled in CASCADE and confirmed using HFSS. Results are plotted in Figure 18. As with the input window, the window is free of any parasitic modes in the operating regions.

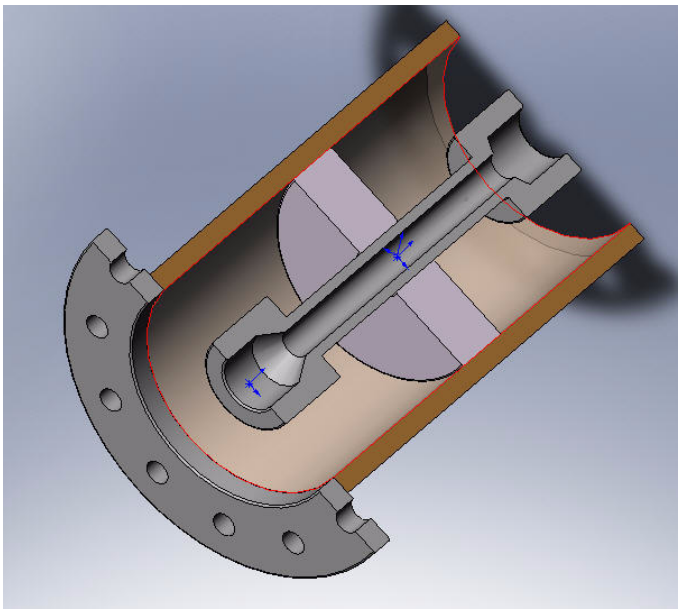

Figure 17. Sliced view of output window

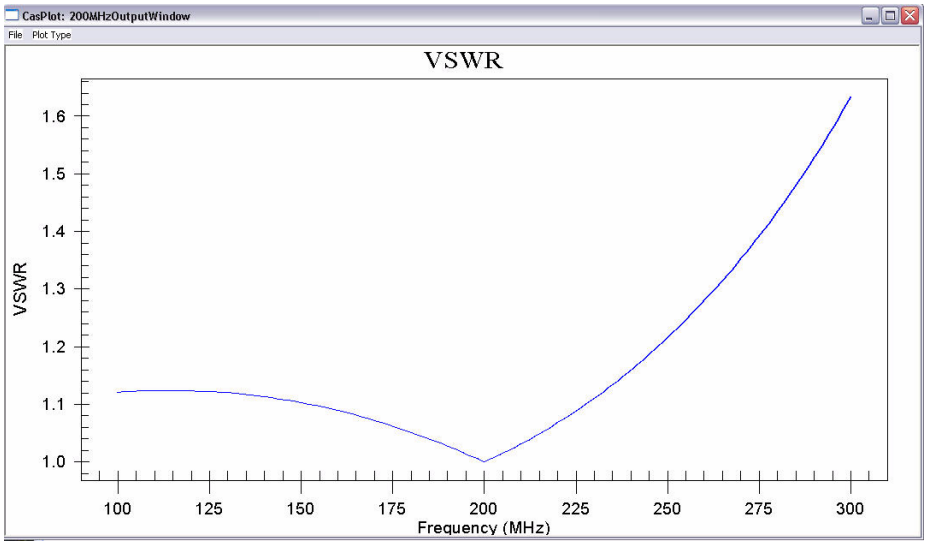

Figure 18. VSWR of output window as modeled in CASCADE (left) and HFSS (right)

2.3.3. Collector

3D computer simulations demonstrated feasibility of a common collector for all twenty four beams. In this simple design, the beams enter a common coaxial enclosure and primarily impact on a downstream wall. Since the purpose was only to demonstrate feasibility, this simple design provides a worst case configuration. In the final design, the walls of the collector will be tapered to provide a slanted surface for impact, increasing the area and reducing the power density. In addition, the collector length will be increased

beyond that used in these simulations. Figures 19 and 20 show simulations of the outer

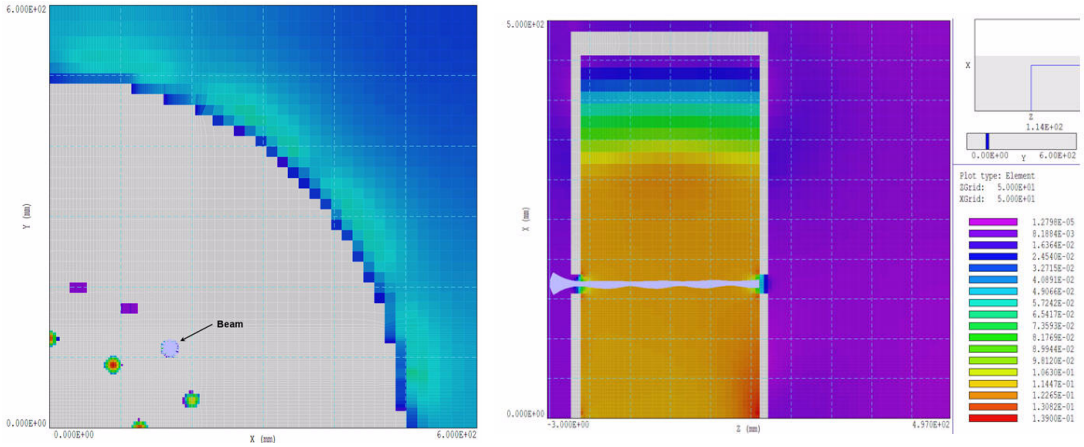

Figure 19. Configuration of outer beam and collector simulation. Left view is 1/4 of the geometry in the transverse plane. The right view is a view of the beam with the axis along the abscissa. Magnetic field values are in Tesla.

electron beams, and Figure 21 shows simulations for the inner electron beams.

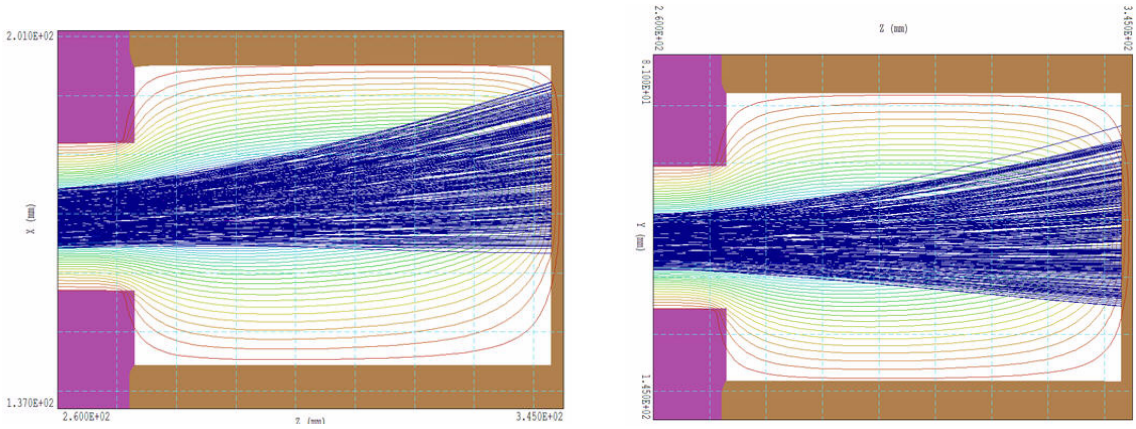

Figure 20. Outer electrons in collector. XZ plane image is on left and YX plane image is on the right.

Never the less, this simple configuration resulted in average collector power densities less than 800 W/cm^2. A power density of 1 kW/cm^2 is typically considered the limit for CW collectors, though IOT collectors dissipating much higher power densities have been developed by CPI, the industrial partner on this program. Simulation of the beam trajectories are presented in Figure 21. Figure 23 shows the corresponding power densities.

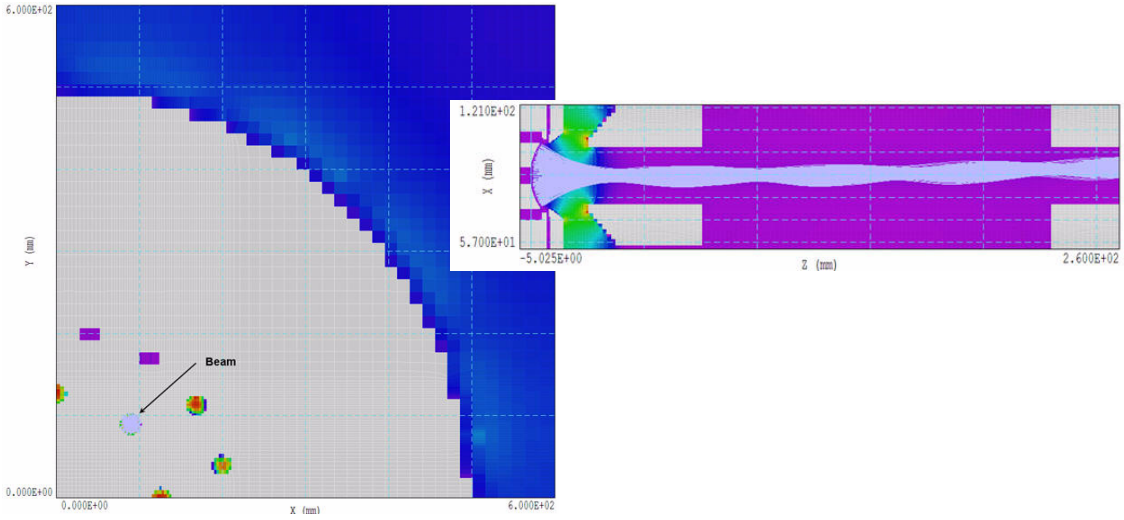

Figure 21. Simulation of inner electron beam in magnet. The left image shows 1/4 of the geometry in the transverse plane. The right figure shows simulation of an inner electron beam.

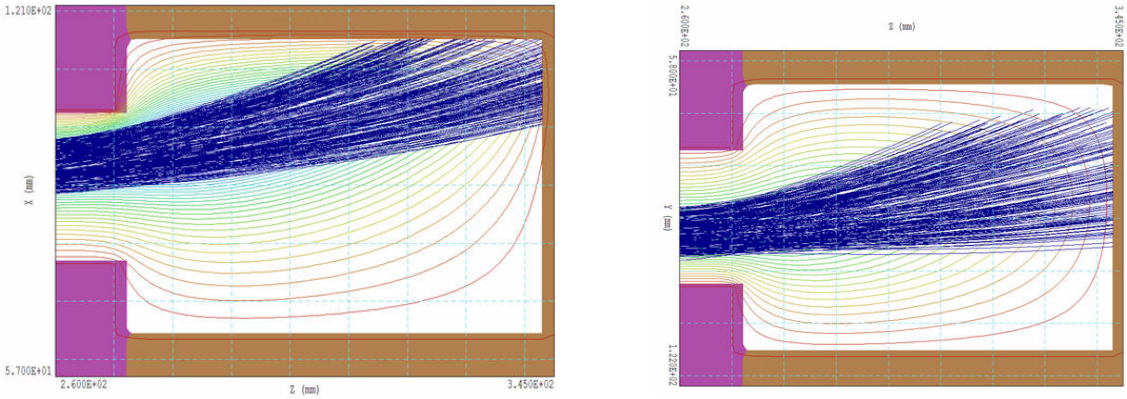

Figure 22. Simulation of inner electron beam in the collector. XZ plane is on the left and YZ plane is on the right.

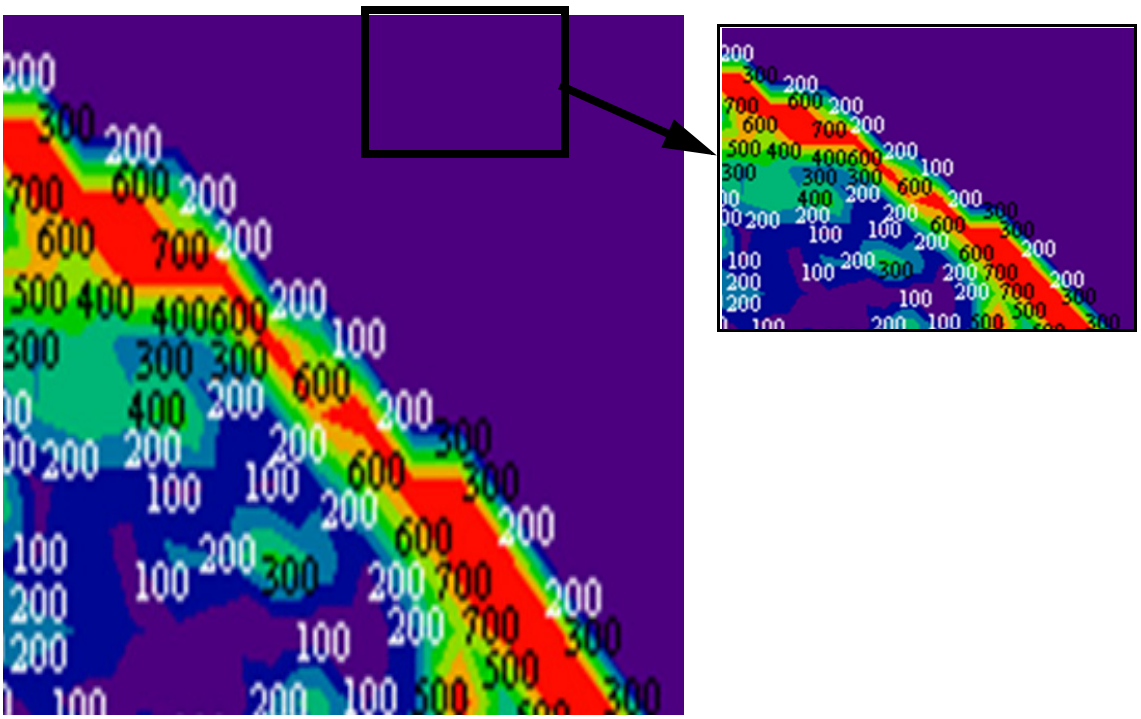

Figure 23. Collector power densities corresponding to analysis shown in Figure 21. Right image is enlarged view of high power density region.

A preliminary solid model of the collector is shown in Figure 24. This shows how the interior walls of the collector will be lengthened and tapered to reduce the peak power density.

Perhaps a more important consideration will be avoiding electron reflection back toward the output cavity. The high efficiency of the output cavity results in slow electrons entering the collector. Excessive space charge in this region can reflect electrons back toward the electron gun. This analysis requires 3D particle in cell (PIC) simulations, which are computationally intensive.

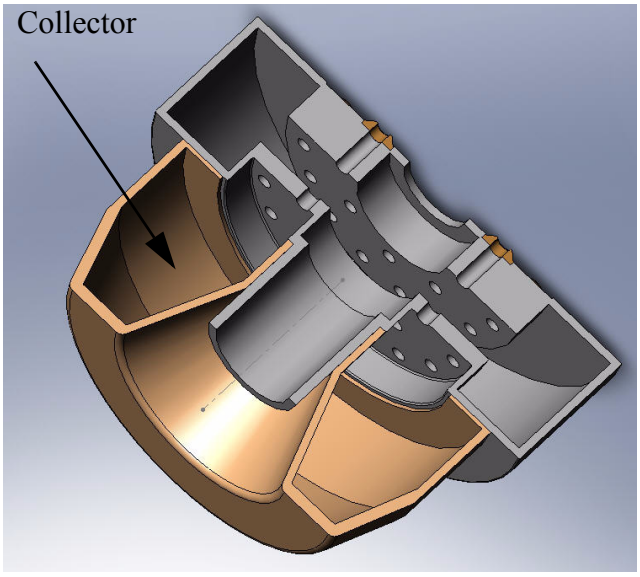

Figure 24. Collector Assembly mounted to output cavity

2.3.4. Magnet

A sliced view of the magnet solid model is shown in Figure 25. This simple design consists of one coil and the surrounding iron forming the outer return path and the input and output polepieces. Openings for the electron beams are indicated.

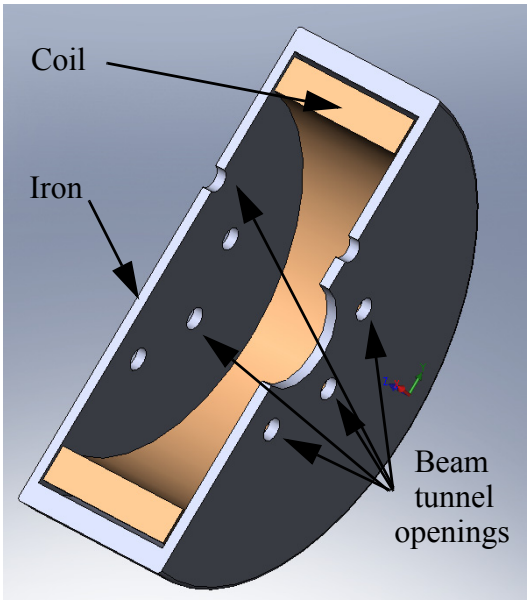

Figure 25. Sliced view of magnet assembly

This geometry creates a flat magnetic field for confinement of the electron beam as it propagates from the gun to the collector. Unlike most linear RF sources, it is not practical or necessary to precisely match the electron beam from the gun into the circuit magnetic field. This is because the beam current is continuously varying during the RF cycle. As long as propagation is achieved for all values of the grid voltage and current, the IOT will operate efficiently. This is a significant advantage over multi-cavity, RF sources which require a high quality electron beam for efficient bunching. In the IOT, the bunch is created directly from the cathode.

2.3.5. Input and Output Couplers

The couplers are integral components in the input and output cavity, so their design occurred in parallel with the cavity designs. The performance predictions provided in Section 2.1 included the couplers. Consequently, those results will not be repeated here.

2.4. Generate a mechanical model of the complete RF source

The complete model of the multiple beam IOT is shown in Figure 26. This figure demonstrates the extreme compactness that makes the IOT an excellent RF source at lower frequencies. Additional reduction in length is achieved with the multiple beam configuration, which also results in dramatic reduction in power supply and support costs. Total length is approximately 80 inches with a maximum diameter of 30 inches. This does not include the magnet assembly. Estimate weight of the MBIOT is 1800 pounds. The magnet is currently estimated

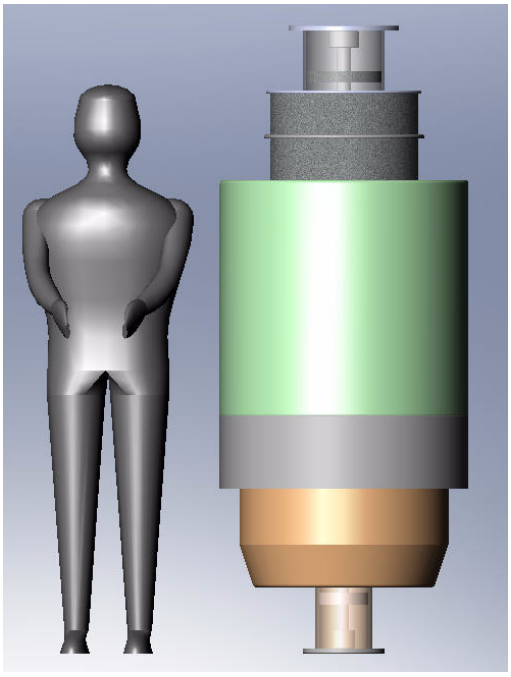

Figure 26. 200 MHz MBIOT model with 6 ft human figure

at 400 pounds. No effort was made during the Phase I program to minimize either size or weight.

Figure 27 shows a sliced view of the complete MBIOT showing major components described above, including the high voltage insulators and input and output flanges. Detailed design of all electrical and cooling circuits and connections were beyond the scope of the Phase I program.

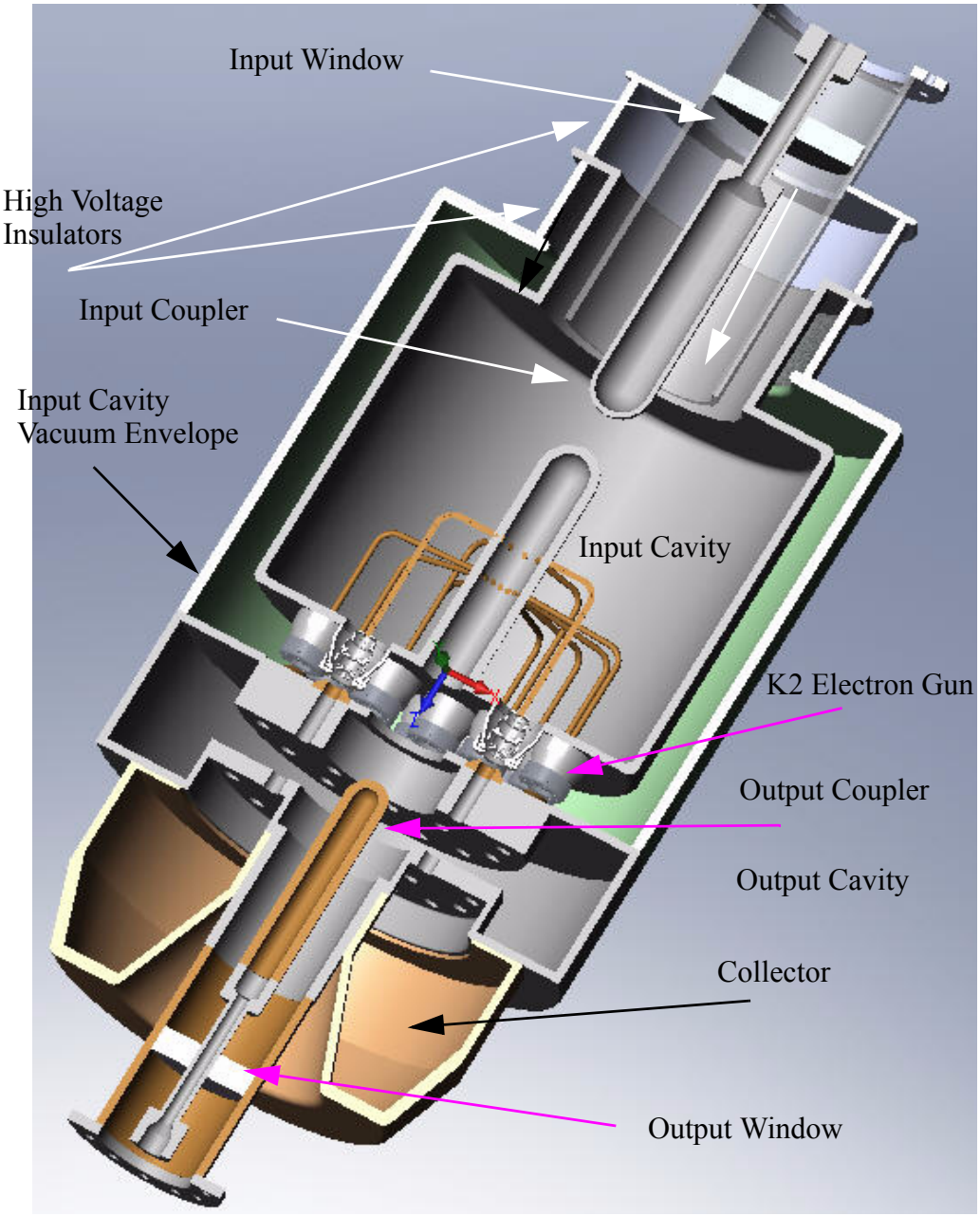

Figure 27. Sliced view of 200 MHz multiple beam IOT solid model

3. Summary

The Phase I program successfully demonstrated feasibility of all major components of the 30 MW, 200 MHz multiple beam inductive output tube. Given sufficient resources, it is very likely that the device could be successfully built and tested.

A problem may exist, however, with the cost. The K2 guns proposed for this device are currently in production at CPI. These are built in relatively high volumes, since the complete line of CPI IOTs use this same gun. The cost for twenty four guns would be approximately $360,000. This would leave approximately $340,000 in a Phase II program to design, fabricate, assemble the remaining components and test the device.

Another serious issue is the driver for the MBIOT. Since the gain is only 24 dB, a 200 kW driver would be required to achieve 30 MW from the final device. The most practical approach may be to develop another IOT at the 200 kW level for the driver. CPI has completed preliminary design for such a device and could complete that development and provide the IOT driver. Their estimated cost, however, is $1.25 million. This price includes non-recurring engineering costs and construction of a non-deliverable prototype in addition to delivery of the final device.

Clearly, design, fabrication, and test of a 30 MW MBIOT, including acquisition of a driver, is beyond the scope of a Phase II SBIR program. A possible approach would be to fund the 30 MW MBIOT in a Phase II program with the driver developed with other funds and provided to CCR as government furnished equipment. Testing would also be an issue for a Phase II program, since it is not readily apparent that test facilities exist for the voltages and impedances required.

4. References

[1] See for example www.arww-rfmicro.com/html/00000.asp

[2] F. Scarpa, A. Facco, V. Zviagintsev*, Z. Lipeng, Ruan Ti, “A 2.5 kW, Low Cost 352 MHz Solid State Amplifier for CW and Pulsed Operation, “Proceedings of EPAC 2002, Paris, France, pp 2314-2316.

[3] Virtual Laboratory Environment for High-Voltage Radiation Sources, U.S. Air Force contract number FA9550-06-C-0081, August 2005 through January 2008.

[4] F. Scarpa, A. Cacco, V. Zviagintsev, Z. Lpeng, “1 2.5 kW, Low cost 352 MHz Solid State Amplifier for CW and Pulsed Operation,” Proceedings of EPAC 2002, Paris, France, pp. 2314-2316.

[5] C. Piel, B. Aminov, A. Borisov, S. Kolesov, H. Piel, “Development of a Solid State RF Amplifier in the KW Regime for Application with Low Beta Superconducting RF Cavities,” Proceed. 2005 Particle Accelerator Conference, Knoxville, TN, 2005, pp. 1-3.

[6] A. Jain, D.K, Sarma, A.K. Gupta, P.R. Hannurkar, “High power solid state rf amplifier for proton accelerator,” Review Sci. Instruments, Vol. 79, Issue 1, pp. 014702-014702-7 Jan., 2008.